Hydroclimatic Reconstructions in the Lower Basin of the Colorado River

by Kiyomi Morino and David Meko,
Laboratory of Tree-Ring Research, The University of Arizona

Table of Contents

[1] 1.Recon.APP_A.pdf
[2] 1.Recon.APP_B.pdf
[3] 1.Recon.APP_C.pdf
[4] 1.Recon.APP_D.pdf
[5] 1.Recon.APP_E.pdf
[6] 1.Recon.APP_F.pdf
[7] 1.Recon.APP_G.pdf
[8] 1.Recon.APP_H.pdf

INTRODUCTION

Hydrologic contributions to the Colorado River between Lakes Powell and Mead are an important consideration in water resource management in the Colorado River basin (Barsugli et al 2010). Several watersheds contribute to Colorado River streamflow along this stretch, including the Paria, Kanab, Little Colorado, Virgin and Muddy. In addition, although its outlet is located below Lake Mead, the Bill Williams River can also impact reservoir operations. For example, during years when Alamo Lake, the flood control reservoir at the head of the Bill Williams River, reaches capacity, excess water can be stored behind Parker Dam on the Colorado River for downstream users. In effect, less water need be released from Lake Mead. While the impact of these Lower Basin watersheds is individually small in comparison to hydrologic contributions of the Upper Basin, collectively, they could delay the decline of reservoir levels for several years. Extra time, if only a handful of years, would allow for the development of more robust responses to water shortages should any arise.

Information on hydrologic and climate variability at various time scales from years to decades to centuries could contribute to a better understanding of possible effects of climate variations on operations. The length of instrumental records for each of these watersheds precludes the characterization of longer-scale variability, namely over multi-decadal to centennial time scales. Tree-ring based reconstructions are a natural choice as proxy data for record extension in this region. Tree-ring reconstructions have revealed important features of pre-instrumental streamflow history the Colorado River (e.g., Stockton and Jacoby 1976; Woodhouse et al. 2006; Meko et al. 2007), and have been applied in assessments of sensitivity of management of the Colorado to climate variation (Prairie et al. 2007; U.S. Bureau of Reclamation 2007).

One of the challenges to streamflow reconstruction in the Lower Basin comes from the hydrologic setting. Short-duration, high-runoff events in semi-arid river watersheds with flashy streamflow regimes may contribute a large proportion of the annual flows without leaving a commensurate imprint on the water balance in the root zone of the tree. Indeed, high annual flows in some years may come from fairly localized precipitation anomalies that might be missed by a sparse tree-ring network. Unlike tree-ring indices, annual flows in such settings are likely to be highly positively skewed. In semi-arid watersheds, it is also reasonable to expect non-linearity in the relationship of annual streamflow to tree-ring indices. For example, precipitation amounts may fluctuate in some dry years within a range where soil moisture and tree-growth is affected but not the runoff at downstream gages.

Most reconstructions have relied on linear regression, sometimes after transformation of flows (e.g., Smith and Stockton 1981; Meko and Graybill 1995; Meko et al. 2001). Within the regression model have been varied approaches to data reduction, heteroskedasticity of errors, lagged responses and predictor-selection. Reconstruction methods were reviewed by Loaciga et al. (1993). Gangopadhyah et al. (2009) review some more recent developments in regression-based streamflow-reconstruction modeling

and introduce a non-parametric approach to streamflow reconstruction that completely obviates the need for regression.

Here, we employ a semi-parametric reconstruction model that can accommodate varying degrees of non-linear relationships between tree-growth and hydroclimate. The model uses robust locally-weighted regression (Cleveland 1979) in a three-stage reconstruction process. The first stage translates individual tree-ring indices into estimates of hydroclimate; the second stage weights those individual hydroclimate-estimates into a single time series; the third stage re-calibrates the weighted time series into a final reconstruction. A similar three-stage approach using conventional least-squares modeling has been used previously in reconstruction of precipitation (Meko 1997) and streamflow (Meko et al. 2007). The model is applied to generate reconstructions of either annual flows (water year) or, when hydrological data are insufficient or otherwise problematic, precipitation. Analysis of the reconstructed hydroclimatologies focuses on drought history. Additionally, for streamflow reconstructions of the Little Colorado and Virgin Rivers, we also examine covariation with both the Colorado and Gila River reconstructions.

Organization of this report

This report contains analyses and data pertaining to hydroclimatic reconstructions of six watersheds in the Lower Basin: the Virgin River, the Little Colorado River, the Paria river, Kanab Creek, the Muddy River and the Bill Williams River. The main body of this report has two objectives. The first is to provide a general overview of the study area and data used, as well as an outline of the technique used to develop these hydroclimatic reconstructions. The second is to analyze larger-scale patterns of temporal and spatial variability by simultaneously considering multiple target watersheds.

Detailed information describing the development and analysis of reconstructions for each of the six target watersheds, as well as reconstruction data in table format, are contained in Appendices A through G. For each watershed, we focused on the characterization of drought occurrence. Extra analyses to further characterize hydrological variability over time and space were conducted for the Little Colorado and Virgin River reconstructions, owing to their larger hydrological contributions to the Colorado River relative to the other target watersheds. And lastly, Appendix H contains Works Cited in this report, including in Appendices A through F.

STUDY AREA

Target Watersheds

This study focuses on six watersheds in the Lower Basin: Little Colorado, Paria[9], Kanab, Virgin, Muddy and Bill Williams (Figure 1, Table 1). The southern-most watershed is

[9] For planning purposes, the Paria is considered part of the Upper Basin. For this study, however, we are treating it as a Lower Basin watershed because the Paria River flows into the Colorado River below Lake Powell.

the Bill Williams; the northern most is the Muddy. The Muddy and Virgin Rivers flow into the Overton Arm on the north side of Lake Mead. The Paria, Little Colorado, and Kanab discharge into the Colorado River between Lakes Powell and Mead. The Bill Williams River flows into the Colorado River south of Lake Mead. Watersheds range in size from 3,700 km^2 (1,400 mi^2) to 68,600 km^2 (29,300 mi^2), for the Paria and Little Colorado, respectively. The Virgin and Little Colorado provide the largest inflows into the Colorado River, with average annual (water year) runoffs of 217.0 mcm (176.0 kaf) and 194.8 mcm (157.9 kaf), respectively. The lowest hydrological contribution to the Colorado River is from the Kanab with an average annual runoff of 10.3 mcm (8.3 kaf). More specific information for each watershed can be found in the respective sub-report for each watershed.

Climatology

Precipitation in the Lower Basin is delivered mainly by cyclonic storms imbedded in the westerlies in the cool-season months, and by convective storms associated with the North American Monsoon (NAM) in summer (Adams and Comrie 1997). Cutoff lows sometimes contribute substantial cool-season precipitation, and moisture from decaying tropical depressions in the Pacific can (rarely) produce substantial precipitation in summer and fall (Smith 1986).

DATA

Hydrologic Data

See sub-reports for individual watersheds.

Precipitation Data

Precipitation variations were characterized with PRISM (Precipitation-elevation Regressions on Independent Slopes Model) data (Gibson et. al 2002). Monthly PRISM data, 1900-2010, for the continental US were downloaded from the PRISM site (http://prism.oregonstate.edu/products/). Data pertaining to each watershed were subsequently "clipped" from the larger dataset using a script written in MatLab ™. In all watersheds, precipitation and hydrological were compared and evaluated for strength of relationship and trends. For watersheds where a streamflow reconstruction was deemed infeasible, either annual (water year) or seasonal precipitation (in mm averaged over watershed) was reconstructed.

Tree-Ring Data.

The majority of tree-ring sites used in the development of hydroclimatic reconstructions of the Lower Basin were obtained from the International Tree-Ring Data Bank (ITRDB) (http://www.ncdc.noaa.gov/paleo/treering.html). Sites with an outer date of 2008 or later were either updates of previously collected sites, or new collections. More details regarding the tree-ring data used in individual reconstructions can be found in sub-reports for individual watersheds.

METHODS

Description of the reconstruction model is deferred to the next section. The same reconstruction model was used for both streamflow and precipitation reconstructions. Individual reconstructions were analyzed using some or all of the following techniques: 1) correlation analysis; 2) assessment of low-frequency fluctuations; and 3) covariation of streamflows. Correlation analysis and significance-testing of correlations follow Snedecor and Cochran (1989), with adjustment as needed for autocorrelation (Dawdy and Matalas 1964). Assessment of low-frequency fluctuations included smoothing by evenly-weighted moving averages (Panofsky and Brier 1958) and Gaussian filters (Mitchell et al. 1966). Covariation of streamflows as a function of frequency was summarized by cross-spectral analysis (Bloomfield 2000). More details on this technique can be found in Meko and Woodhouse (2005). These analyses can be found in the individual reports for each watershed.

Streamflow into Lake Mead

We estimated the temporal variability of hydrologic contributions into Lake Mead by summing reconstructed streamflows. In this analysis, we used only the reconstructions of the Virgin and Little Colorado Rivers because data limitations precluded hydrologic reconstructions of the Paria, Kanab, and Muddy watersheds (instead, precipitation was reconstructed). For this set of watersheds, these two rivers likely provide a robust representation of between-reservoir water supply given that the contributions of the Virgin and Little Colorado Rivers are disproportionately high compared to the Paria, Kanab and Muddy. Average annual (water year) flows sum to 411.7 mcm (333.8 kaf) for the Virgin and Little Colorado compared to 73.1 mcm (59.3 kaf) for the Paria, Kanab and Muddy.

Hydroclimatic variability across watersheds

We compared decadal patterns of Lower Basin hydroclimatology as they vary over space. In this analysis, we converted each of the six reconstructions, as well as the Colorado River (Meko et al 2007) and Gila River (Meko) reconstructions, to z-scores and smoothed the data using a 21-year Gaussian filter. The period of comparison was 1400-2010 for unsmoothed data. Dry conditions were defined by periods during the reconstruction when z-scores for streamflow, or precipitation, were less than the 20^{th} percentile. Wet conditions were defined by periods during the reconstruction when z-scores for streamflow, or precipitation, were greater than the 80^{th} percentile. These analyses can be found at the Results and Discussion section of this document.

Reconstruction Model

Tree-Ring Standardization. Ring widths were initially screened to eliminate any series shorter than 150 years. This step counters the so-called "segment-length" curse, a loss of low-frequency variability sometimes incurred when site chronologies are formed by averaged over individually detrended short series (Cook et al. 1995). The

standardization of remaining ring widths into dimensionless tree-ring site chronologies broadly followed Cook et al. (1990a,1990b). For removal of age-related or size-related trend in mean ring width, a cubic smoothing spline with a frequency response of 0.95 at twice the series length was fit to each core ring-width series. The core index was then computed as the ratio of ring width to the fitted curve. This procedure allows retention of considerable variability at wavelengths shorter than the series length in the index.

Short-term persistence was then removed from the core indices by autoregressive (AR) modeling. This step was deemed necessary because exploratory analysis showed the persistence in the core indices varied greatly from tree-to-tree and was typically much higher than that of either annual precipitation or the annual streamflow series to be reconstructed. The order of AR model – up to order 3 – was selected by a modified Akaike Information Criterion (Hurvich & Tsai 1989).

Before averaging core indices into site chronologies we also removed possible age-related or size-related trends in variance by a method described in detail elsewhere (Shiyatov et al. 1990; Meko et al. 1993). This method essentially consists of removing trend in absolute departures from the mean from the core indices. Core indices at each site were next averaged to generate a preliminary site tree-ring chronology. The chronology was truncated at the early end, if necessary, to eliminate the part of record with insufficient common signal, as indicated by a subsample signal strength (SSS) lower than 0.85 (Wigley et al. 1984). Finally, the site chronology was variance-stabilized as recommended by Osborn et al. (1997) to adjust for possible changes in variance related to time-varying sample size.

Single-Site Reconstructions. The first stage of modeling was conversion of each tree-ring chronology into a separate estimate of hydroclimate (streamflow or precipitation), referred to as a single-site reconstruction (SSR). The conversion was achieved through scatterplot smoothing with the aid of robust locally weighted regression (Cleveland 1979). The basic scatterplot for this conversion is a plot of observed hydroclimate on the tree-ring index for the common period of the two series. The regression was applied to windowed neighborhoods of points defined by locations along the predictor axis. For the scatterplot of $\{x,y\}$ points, where x is the tree-ring index and y is hydroclimate, a local linear (first-order polynomial) model was used to generate estimates of flow at 11 abscissa points: the minimum, 0.10, 0.20… 0.90 quantiles, and maximum of x. Locally weighted regression minimizes a weighted function of the squared residuals, with lower weights assigned to points whose x-values (x is the predictor) are further from the point x_0 defining the center of the estimation neighborhood. Robust locally weighted regression extends this procedure by iteratively adjusting the weights depending on the residuals, and is aimed at reducing the impact of outliers on the regression. Following Martinez and Martinez (2002) we used a tri-cube function in weighting the points for localized regression, and the bi-square function for the robustness weights.

Once estimates of hydroclimate were obtained for the 11 abscissa target points, straight-line segments were drawn connecting the estimated hydroclimate. The joined segments form a smoothed scatterplot, which is also referred to as a "loess" curve (Cleveland et al.

1984). The two parameters in the fitting of the loess curve are the order of the polynomial and the smoothing parameter, α. As we decided a-prior on the local-linear model, the only variable parameter for our model was α, which specifies the size of the "local" neighborhood to be used in fitting. If the total number of observations in a scatterplot is N, the subset used is roughly αN. As α increases, the loess curve becomes smoother but tracks the observations less closely. We set the final value of α by the following iterative procedure. The parameter α was initially set to α=0.2 and was increased in increments of 0.05 until the loess curve became monotonically increasing. The monotonic constraint is consistent with a conceptual model that increasing tree-ring index goes with increasing flow. If the resulting loess curve still had a jagged appearance after first becoming monotonic, α was further increased, but only as long as the variance of flow explained by the loess curve dropped by no more than 1 percent below that of the first monotonically increasing curve. Estimates of hydroclimate for each year's tree-ring index in the calibration period were then made by linear interpolation onto the loess curve. Variance explained was computed as,

$$R^2 = 1 - \frac{SSE}{SSY} \qquad (0.1)$$

Where *SSE* is the sum of squares of residuals of observed and estimated hydroclimate , and *SSY* is the sum of squares of departures of observed hydroclimate from its mean for the period of the scatterplot.

The SSR models were validated by both split-sample validation (Snee 1977) and cross-validation (Michaelsen 1987). A chronology was dropped from the modeling if $R^2 < 0.10$ in cross-validation or if the reduction-of-error (RE) statistic (Fritts et al. 1990) was negative for either half of the split-sample validation.

The final step in generating the SSRs from the model was to interpolate hydroclimate for the entire length of the tree-ring index by linear interpolation onto the loess curve. The only complication to this interpolation is when a tree-ring index falls outside the range of index encountered in the calibration (scatterplot) period. We dealt with this problem, both in the cross-validation exercise and in the long-term reconstruction, by linearly extending the loess curve as needed. At the high end, the line segment joining the hydroclimate estimates at the 0.90 quantile and the maximum calibration-period index was extended to the global maximum index, the largest index in the full-length tree-ring series. An analogous extension was made at the low end of the loess plot.

Weighting of SSRs. Consider a subset of *m* years of the tree-ring record covered by some subset of *n* SSRs. The first principal component from a PCA on the covariance matrix of those *n* SSRs for the *m*-year period was used as a weighting function to combine the hydroclimate signals from the various chronologies. The scores of PC#1were then defined as a new predictor combining flow information from multiple tree-ring sites.

Recalibration and Reconstruction. The scores of PC#1 from the previous step were recalibrated into estimates of hydroclimate by loess modeling following the same criteria

for selection of smoothing parameter as used in the SSR models. The only difference in the two phases of modeling is that for the SSRs the smoothed scatterplots are hydroclimate against tree-ring index while for the final reconstruction model the scatterplots are hydroclimate against the scores of PC#1 of the SSRs.

Uncertainty. For the Paria River, Kanab Creek, the Muddy River and the Bill Williams River, uncertainty was discussed in term of validation statistics. For the Virgin and Little Colorado River streamflow reconstructions, uncertainty was summarized by the cross-validation residuals of the final loess model. The root-mean-square error (RMSE) of those residuals was computed as a single measure of uncertainty. Recognizing that the error variance may not be constant over the full range of reconstructed flows, we also computed an empirical 50 percent confidence interval conditional on the magnitude of reconstructed flow. The steps were (1) build a sequence of cross-validation residuals by successively fitting the loess model, each time leaving out one observation and using the loess curve to estimate the flow the omitted observation, (2) stratify the cross-validation residuals as dry-year, normal-year or wet-year depending on the tercile of reconstructed hydroclimate, (3) compute the median absolute positive residual and median absolute negative residual for each tercile subset of observations, and (4) define the 50% confidence interval for any reconstructed hydroclimate $\hat{y}_t$ as $\hat{y}_t - c_N$ to $\hat{y}_t + c_P$, where c_N and c_P are the median absolute negative and positive residuals for the tercile into which $\hat{y}_t$ is classified. This method in principal follows the "upper and lower smooths" technique described for confidence intervals of loess-model estimates by Cleaveland and McGill (1984) and Martinez and Martinez (2002).

Sub-period modeling and blending. The steps described above constitute development of a single reconstruction model, and apply to SSRs based on a specific group of tree-ring chronologies with some common time coverage. Because some years of tree-ring record may not be represented by all of the chronologies in some ideal group, it can be useful to generate multiple reconstructions based on different tree-ring subsets and then splice the various versions together to get a final reconstruction with longest possible time coverage (e.g., Meko 1997; Meko et al. 2007; Cook et al. 2007). We used such a "time-nested" modeling approach. We identified useful subsets of tree-ring chronologies from an exploratory correlation analysis that included PCA separately run on every unique combination of SSRs represented in the years of the tree-ring record. The correlation of hydroclimate with the scores of PC#1 was used as a guideline for strength of tree-ring set; some preference was also given to sets with a larger number of chronologies. Several subsets were selected and the steps listed in previous sections were repeated to get multiple reconstructions with differing accuracy and time coverage. Reconstructions were then spliced, with priority in order of decreasing cross-validation RMSE of the model.

RESULTS AND DISCUSSION

Lake Mead Inflow

Combined streamflow of the Virgin and Little Colorado Rivers averages 360 kaf (445 mcm) for the period of analysis (1496 – 2008). The distribution of combined streamflows is positively skewed (skew = 1.44) and significant at $p<.05$. These two rivers combine for a total between 250-500 kaf over half the time during the five-century reconstructed record (Figure 2A). Larger volumes, those greater than 500 kaf, occur about 15 percent of the time. The highest combined flow for these two rivers was 1,068 kaf in 1594 (Figure 2B). In only two other years did streamflow total to more than 1,000 kaf: 1849 and 1862. For a 30-year moving window of years when streamflow was greater than 500 kaf, the maximum frequency was 10 years, during the 1700s (Figure 2C). Indeed, the 1700s stand out as a period of relatively high frequency of high-flow years; whereas the 1500s and 1600s are notable for the low frequency of high flow years (Figure 2B).

Our findings indicate that streamflow into Lake Mead below Lake Powell, generally, is relatively low but punctuated by years of very high inflow. Extreme high flow events are likely underestimated by the tree-ring record because annual tree growth tends to be a poor indicator of short-duration, high-runoff events. A recent example serves to illustrate this point. In January 2005, the Littlefield gage on the Virgin River recorded a peak discharge of 37,000 cfs, the largest on record. This was followed by five months of much higher than average flow, leading to an annual (water year) total of almost 600 kaf; whereas, reconstructed flow for this year was just over half this amount, 324 kaf.

Lower Basin Hydroclimatic Variability

Dry spells. Figure 3 shows the distribution over time and space of periods during the reconstruction when streamflow, or precipitation, was less than the 20^{th} percentile. Several patterns emerge. First, drought frequency and duration in the Virgin, Kanab, and Paria show high levels of similarity (Figure 3 C,D&E). In particular, there is a very strong synchronicity of drought during the 1700s and late 1800s. The striking covariation amongst these three watersheds is attributable to the high degree of overlap in the tree-ring sites used for the development of each of the reconstructions. However, there is also a hydroclimatological interpretation of this pattern. The regions of greatest moisture supply for each of the watersheds, i.e., the highest elevations, are located in close proximity to each other. Moreover, winter precipitation which figures strongly in each of the reconstructions tends to be generally homogeneous over space.

In the more southerly watersheds of the Lower Basin - the Little Colorado, the Bill Williams and the Gila, there are also strong similarities in drought occurrence during the period of overlap (Figure 3 F-H). After the mid-1600s, seven dry periods occur with roughly the same timing and for the same duration in all three watersheds. Prior to ca. 1600, the Little Colorado and Gila show distinct differences in drought occurrence; whereby, drought was more frequent in the Little Colorado. Again, there is some overlap in the sites used to develop the Little Colorado and Gila River reconstructions. But, like the more northerly set of Lower Basin reconstructions, the close proximity of headwater

regions and spatial homogeneity of winter precipitation can account for these similarities. Differences between the southern and northern group include a drought occurring ca. 1700 and the 1930s; whereas, these droughts occur in the northern group, they are absent in the southern group. There is also a dry spell in the early 1600s that occurs in the Muddy, Virgin and Paria, as well as in the Colorado River reconstruction, but not in the Little Colorado, Bill Williams or Gila.

For the entire Lower Basin, (Figure 3 B-H), the earliest widespread dry period was the late 1500s. This feature also appears in the Colorado River reconstruction (Figure 3A), indicating this drought was spatially expansive. Other widespread dry spells include events in the late 1600s, late 1700s and late 1800s, as well as the 1950s. Drought was conspicuously absent in both Upper and Lower Basins during a large portion of the 1800s.

Wet spells. Figure 4 shows the distribution over time and space of periods during the reconstruction when streamflow, or precipitation, was greater than the 80^{th} percentile. The Virgin and Paria show high levels of similarity in the timing and duration of wet periods (Figure 4 C&D). And unlike the pattern of dry periods, the Kanab shows a somewhat different pattern from its neighbors (Figure 4 C-E). In particular, apart from one wet episode at the beginning of the 1700s, there are no pluvials from the mid-1600s through to the end of the 1800s. In addition, the wet spell at the beginning of the 1600s is much longer in the Kanab compared to the Virgin and Paria watersheds. Indeed, it is the longest wet period for all reconstructions (Figure 4)

In the Little Colorado and Gila watersheds, wet spells after 1700 occur with similar timing but tend to last slightly longer in the Little Colorado (Figure 4 F&H). Prior to 1700, there are no similarities in the occurrence of wet periods between the Little Colorado and the Gila watersheds. Only one pluvial occurred during this period in the Little Colorado Basin; whereas six occurred in the Gila. Indeed, for all reconstructions, the Little Colorado hosts the longest period without a wet spell, about two and half centuries, ca. 1470 to ca. 1720; the second longest period without a wet spell occurs in the Kanab where there is about a one and a half century period without multi-year wet conditions, ca. 1730 to ca. 1890. Compared to the Little Colorado and the Gila, there are fewer wet spells in the Bill Williams watershed.

For all Lower Basin reconstructions, there is high synchronicity of wet periods during the 1900s. All watersheds indicate wet conditions at the beginning and end of the twentieth century. These two pluvials also occur in the Colorado River reconstruction (Figure 4 A). A couple of short-duration episodes occur at the beginning of the 1700s and are relatively widespread, each occurring in seven of the eight reconstructions. Apart from these, there are few other widespread wet events. There is a wet period during the late 1500s-early 1600s in all watersheds except the Little Colorado but it varies in both timing and duration. Prior to 1600, the Colorado and Gila Rivers show a striking similarity in the occurrence of wet periods; these events are absent in the other long reconstruction, the Little Colorado.

Summary

Several multi-century reconstructions were developed for the Lower Basin. Either streamflow or precipitation was reconstructed, depending on the quality and quantity of hydrological and tree-ring data. An analysis of potential hydrologic contributions from the Virgin and Little Colorado Rivers to Lake Mead indicate that about 15% of the time these rivers can provide pulses greater than 500 kaf. Current estimates of historical (pre-instrumental) flow on these two rivers are derived from Upper Basin water supply patterns. The increased level of accuracy provided by tree-ring reconstructions of each of these rivers could prove useful in fine-tuning long-term management actions in the Colorado River Basin.

An analysis of hydroclimatic anomalies showed a generally high level of similarity for decadal-scale patterns of dry periods. There is one synchronous dry spell per century occurring in at least seven of the eight reconstructions. Sub-regional differences in a dry spells include events in the early 1600s, ca. 1700, and 1930s which occur only in the northern part of the Lower Basin. Compared to dry spells, the occurrence of wet spells in the Lower Basin and Colorado River reconstructions appears to be less synchronous, both sub-regionally and regionally; moreover, there are longer periods without wet conditions occurring in some of the reconstructions.

From a methodological perspective, we have demonstrated the usefulness of a simple scatterplot-smoothing model applied in a three-stage reconstruction procedure. This approach is likely most useful when the relationship between flow or precipitation and tree-ring indices is nonlinear and highly variable both in form and strength among tree-ring chronologies. Using this approach greatly improved the relationship between streamflow or precipitation and tree-ring indices in some but not all cases. Very flashy flows, resulting from the delivery of very high volumes of moisture over a short period of time remain a challenge for hydroclimatological reconstructions. Strength of the approach are that no specific mathematical model is imposed on the relationship between tree-ring index and flow, and that graphical and statistical diagnostic information on site-to-site differences in relationship is available through the SSR models.

TABLE

Table 1. Size and runoff characteristics of the six target watersheds.

Watershed	**Size km^2 (mi^2)**	**Mean annual (water year) runoff mcm (kaf)**
Muddy	18,700 (7,200)	37.7 (30.6)
Virgin	15,000 (5,800)	217.0 (176.0)
Kanab	6,100 (2,400)	10.3 (8.3)
Paria	3,700 (1,400)	25.1 (20.4)
Little Colorado	68,600 (29,300)	194.8 (157.9)
Bill Williams	13,000 (5,000)	128.3 (104.0)

FIGURES

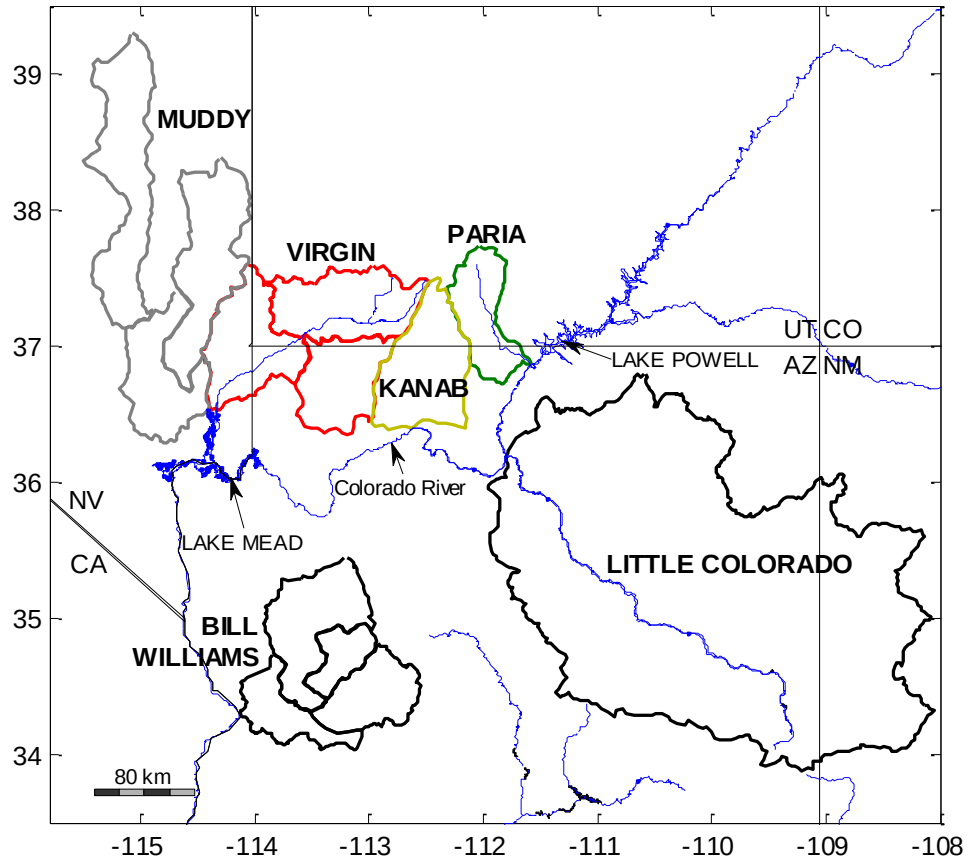

Figure 1. Study area map.

The six Lower Basin watersheds for which hydroclimatic reconstructions were developed.

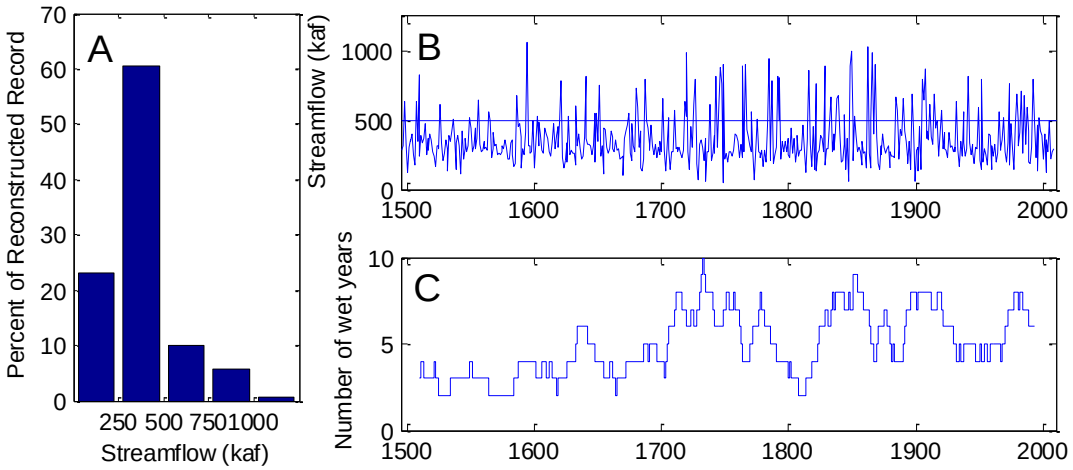

Figure 2. Temporal patterns of the Virgin and Little Colorado Rivers.

Variability of combined streamflow for the Virgin and Little Colorado Rivers over the reconstructed record. A. Bar chart summarizing distribution of streamflows; B. Time plot of annual reconstructed streamflow; C. Time plot of wet-year frequency for a 30-year moving window.

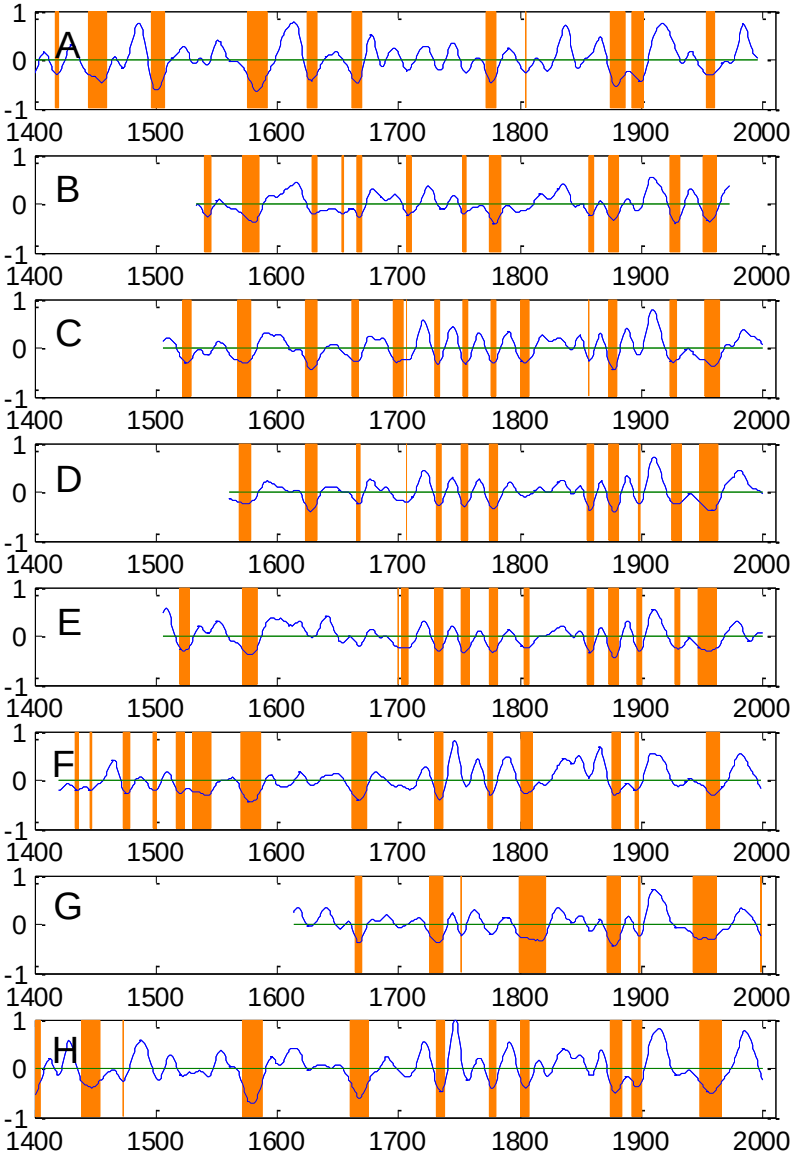

Figure 3. Inter-basin comparisons of dry episodes.

Comparison of dry anomalies (< 20th percentile of z-scores) across reconstructions of streamflow and precipitation. All reconstructions were smoothed with a 21-year Gaussian filter to emphasize decadal-scale variability. A. Colorado River: water year streamflow; B. Muddy River watershed: water year precipitation; C. Virgin River: water year streamflow; D. Paria River watershed: winter precipitation; E. Kanab Creek watershed: winter precipitation; F. Little Colorado River: water year streamflow; G. Bill Williams watershed: winter precipitation; H. Gila River: water year streamflow.

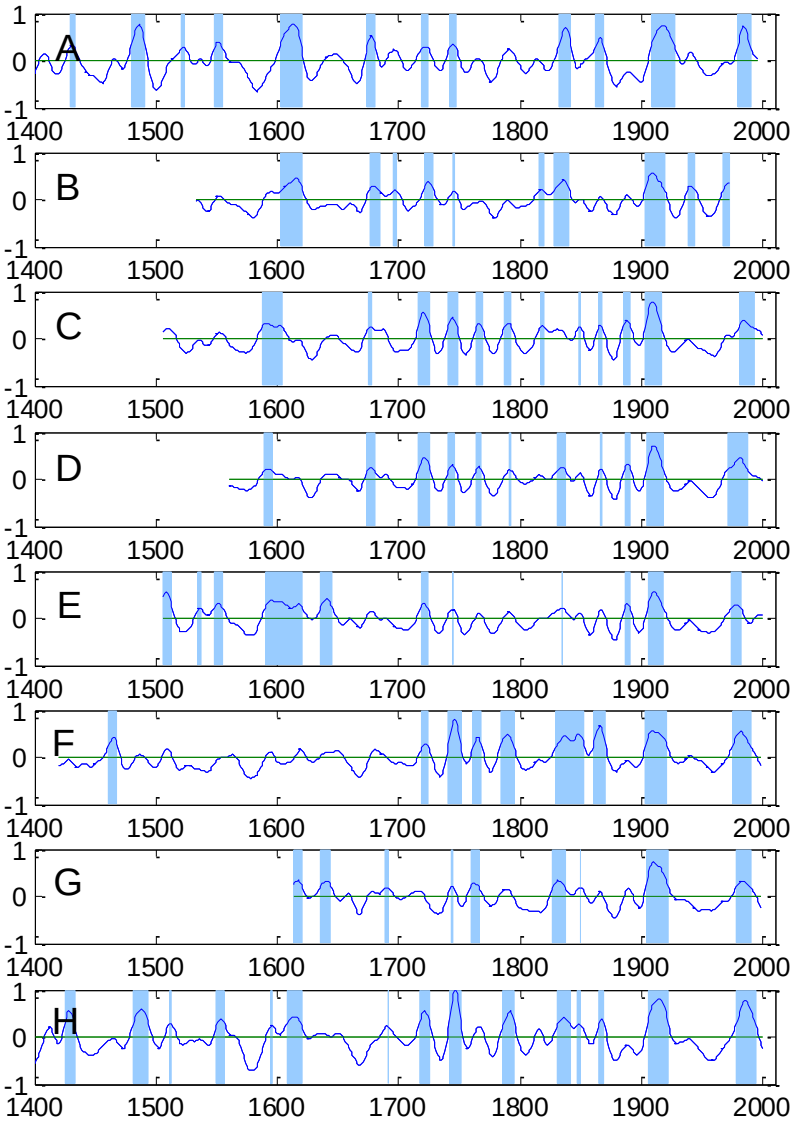

Figure 4. Inter-basin comparisons of wet episodes.

Comparison of wet anomalies (> 80th percentile of z-scores) across reconstructions of streamflow and precipitation. All reconstructions were smoothed with a 21-year Gaussian filter to emphasize decadal-scale variability. A. Colorado River: water year streamflow; B. Muddy River watershed: water year precipitation; C. Virgin River: water year streamflow; D. Paria River watershed: winter precipitation; E. Kanab Creek watershed: winter precipitation; F. Little Colorado River: water year streamflow; G. Bill Williams watershed: winter precipitation; H. Gila River: water year streamflow.